UNIVERSITY OF TURKU

Laser Powder Bed Fusion of copper alloy-based multi-materials: Manufacturing and process optimization

A Literature Review

Department of Mechanical Engineering

Bachelors thesis

Author:

Kalle Laurikainen

16.5.2025

Turku

Bachelor's thesis

Subject: Mechanical Engineering
Author: Kalle Laurikainen
Title: Laser Powder Bed Fusion of copper alloy-based multi-materials: Manufacturing and process optimization
Supervisor: Nikhil Kamboj
Number of pages: 23 pages
Date: 16.5.2025

Style of the abstract is **Abstract**.

Key words: Multi-material, additive manufacturing, powder bed fusion, copper alloy, process optimization

Table of contents

Abstract

The advancement of multi-material additive manufacturing, particularly through laser powder bed fusion, presents significant potential for additive manufacturing. New technologies could enable production of copper alloy-based parts with enhanced mechanical and thermal functionality. This literature review investigates the current state of copper alloy/metal multi-material fabrication, focusing on the challenges of interfacial bonding, material compatibility, and process optimization. Copper alloys such as CuCrZr and Cu10Sn have been identified as promising candidates for integration with an assortment of steels due to their favorable laser absorption properties compared to pure copper. Despite successful demonstrations, manufacturing challenges persist, particularly due to copper's high reflectivity and thermal conductivity. Key strategies, such as process parameter-, post-processing and scanning strategy optimization were analyzed across various studies. Effective interfacial bonding has been achieved through a multitude of techniques such as compositional gradient transitions, strategic scan path planning (e.g., staggered island and interlayer rotation), and post-processing heat treatments such as hot isostatic pressing and age hardening. Notably, this review highlights the lack of comprehensive research on wider array of material combinations. Additionally, porosity, surface roughness, and mechanical strength varied significantly across case studies depending on processing strategies and material combinations.

1 Introduction

Complex part manufacturing is key in many industrial fields where a parts weight to its structural- and thermal properties-ratio is extremely important, for example in aerospace applications. Multi-metal part manufacturing with Laser-Assisted Powder Bed Fusion (PBF-LB/M), offers a promising solution by enabling the production of components made of different materials to serve different functions, such as durability, strength, thermal and electrical conductivity. These types of multi-materials are often referred to as functionally graded materials and are characterized as materials, which's properties gradually change within the part to serve multiple functionalities. An example is circuitry, where copper could be deposited onto ceramics or polymers enabling the printing of entire electrical devices directly [1].

As additive manufacturing continues to revolutionize the production of high-quality, easily designable components, the integration of multiple materials offers new possibilities. This approach enables the fabrication of parts with layered compositions or even multiple materials within a layer. For instance, the thermodynamic properties of copper can be incorporated to function as a heat sink while maintaining a hard outer shell made of stainless steel. However, processing pure copper in PBF-LB/M poses a challenge due to its high reflectivity and thus poor laser absorptivity, requiring the use of high-power lasers to counter. This has been combatted with by using copper-based alloys, such as CuCrZr and Cu10Sn to aid in ensuring a predictable melt-pool and sufficient melting. PBF-LB/M has been seen as a viable process to manufacture Copper Alloy (CuA) based metal multi-materials due to advantages in manufacturing high-resolution parts with high relative density in cost of large size limitation, low build rate and complicated powder delivery which can lead in more material wastage [2].

This thesis aims to enhance the understanding of effective methods for manufacturing CuA-based multi-material components using the PBF-LB/M process. In addition, suggestions for future research are presented. Fig 1. showcases the to path in analyzing literature to examine various metal combinations, processing techniques, treatments, and material properties. The review focuses on methods to help better interfacial bonding strength and part quality of processable multi-materials.

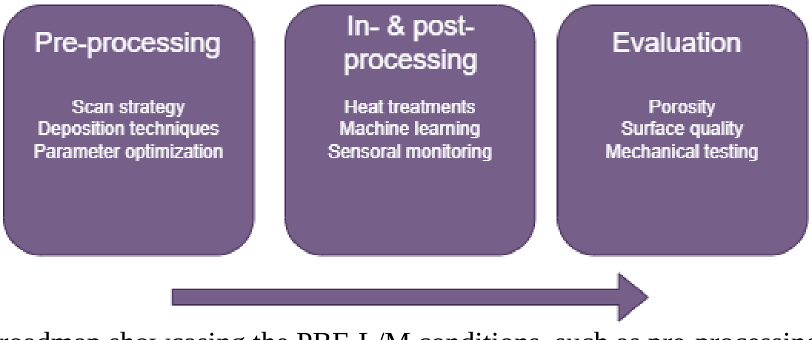

Figure 1. Thesis roadmap showcasing the PBF-L/M conditions, such as pre-processing, in- & post-processing and part evaluation.

2 Copper alloy based multi-materials via PBF-LB/M

Currently, pure copper and its alloys are widely paired in multi-materials and are used in the nuclear and aerospace industries due to their thermal properties. However, as a relatively new and costly technology, the adoption of PBF-LB/M for manufacturing multi-materials remains a challenge for many companies. Despite this, its implementation is becoming more feasible with the increasing knowledge of multi-powder depositing systems [1].

2.1 Overview of the PBF-LB/M process

The PBF-LB/M process (same concept as Selective Laser Melting or SLM) consists of layer by layer melting of deposited material in one or more dimensions.

2.1.1 Key process parameters

Key process parameters in PBF-LB/M processing include laser power P (W), scanning speed v (m/s, laser hatch space T (mm) and layer thickness h (mm) and an indicative ratio between them volumetric energy density (VED), as listed in Table 1. A study preparing 316L/CuSn10 samples found that laser power and scanning speed were the most prominent parameters on fusion-zone width with hatch space having almost no effect [3].

Key parameters		
P	Laser Power	
v	Scanning speed	
T	Hatch space	
h	Layer thickness	
VED	Volumetric Energy Density	$VED = \frac{P}{vTh}$

Table 1. Key parameters in PBF-LB/M processing

2.1.2 Laser absorptivity

A blue or green laser (λ=430nm, λ=515nm respectively) showed significantly increased absorptivity in copper-based materials compared to near-infrared (λ=1064nm). When using Lambda spectrometry, study results showed that a blue diode laser (λ=450nm) had six times greater absorptivity than infrared laser (λ=915nm) [4].

By modifying the surface of powdered metal particles, laser absorptivity can be enhanced. For example oxidizing or carburizing the powder was shown helpful to increase the absorptivity of the laser with cost of decreasing relative density and producing lack-of-fusion defects [4].

2.1.3 Powder feed systems

With most powder feed systems being single-feed, dual feed systems could help premix powder when compositional grading transitions could be beneficial. In addition, dual feed systems could reduce wasted powder from cross contamination. Current PBF-LB/M processes that use flat-bed powder spreading are limited for single material per layer [5]. Ultrasonic assisted powder delivery and powder vacuums can be adopted to feed systems for full control of deposited powder, even though vacuuming a powder presents a large economical and sustainability problem due to unavoidable cross contamination. Ultrasonic assisted multiple powder dispensing has been utilised in PBF-LB/M multi-material manufacturing, for example to fabricate titanium alloy-copper alloy multi-material samples [6].

2.1.4 Scanning strategies

Basic (single-direction, dual-direction- and spiral scanning), two-dimensional (plane-, strip- and island-scanning) and interlayer scanning strategies (interlayer staggered- and orthogonal scanning) are often used in PBF-LB/M processing [1]. Single-direction (a), dual-direction (b), island-scanning (c) and interlayer staggered-scanning (d) showcased in fig. 2.

A study producing 316L/CuSn10/18Ni300/CoCr multi-materials, island scanning was suggested to reduce temperature gradient during the PBF-LB/M process, thereby reducing residual stress and ensuring good interfacial bonding strength [1], [7].

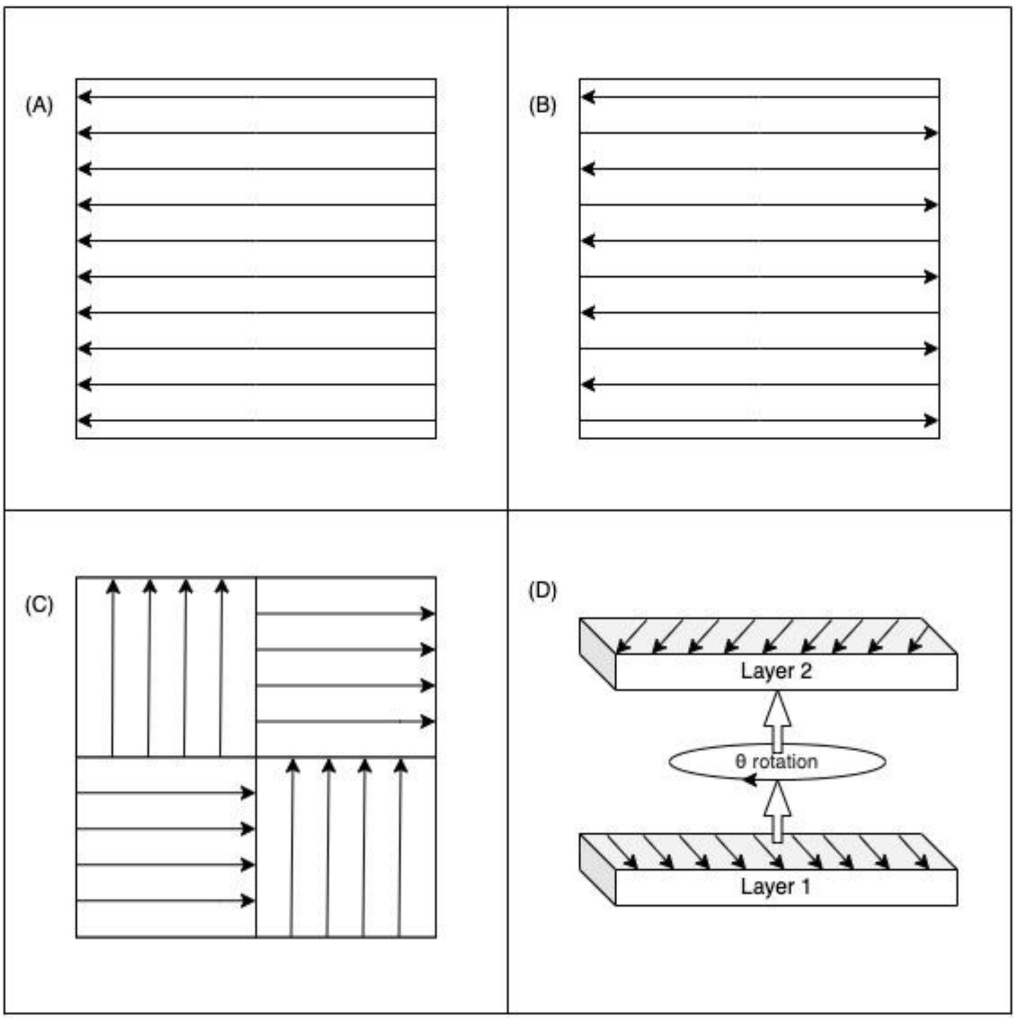

Figure 2. Scanning strategies: A) Single track scanning B) Multitrack scanning C) Island Scanning D) Interlayer rotation by angle θ.

2.1.5 Classification of Multi-material Components

The classification of multi-material components can be broadened to discrete and graded 2D and 3D multi-materials shown in Fig 3. Discrete and graded multi-materials differ in transition between the used materials where ones change in material in contrast to previous layer is discrete and others has been transitioned, respectively [8]. 2D and 3D multi-materials differ in intralayer material deposition where one has material transition in one dimension and other at least in two dimensions, respectively [8].

2D multi-material part manufacturing is the process of applying a single layer of single material and fusing it to another layer of a different material. This is generally easier than 3D manufacturing and could be adopted more easily to already existing PBF-LB/M machinery by switching printable materials.

3D multi-material parts where multiple materials are printed within a single layer are possible to manufacture, while complicated. For example in a study where 4340 steel was printed with CuSn10 on the same layer [1]. This often needs a specialized roller deposition system for multi-powder feed.

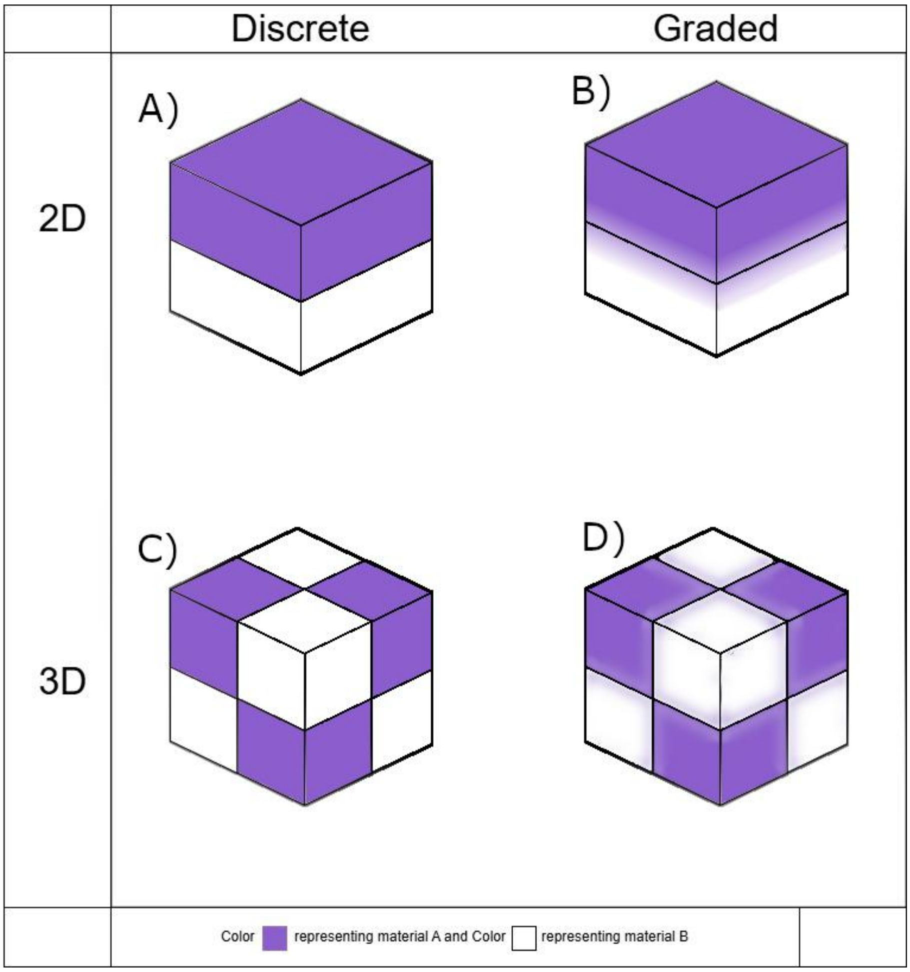

Figure 3. Classification of multi-materials with different colors representing different materials. A) Discrete 2D sample B) Graded 2D sample C) Discrete 3D sample D) Graded 3D sample.

3 Optimizing Part Quality: Current Research and Strategies

3.1 Material Combinations for PBF-LB/M

The most widely used copper alloys in PBF-LB/M processes are CuCrZr alloys and Cu10Sn, especially combined with steels such as 316L, 1.2344 and M300.

3.1.1 CuCrZr

A comprehensive review of CuCrZr alloys processed via PBF-LB/M has highlighted strategies to enhance absorptivity. One approach involves using physical vapor deposition (PVD) to coat pure copper powder with CrZr, which improves the laser absorption efficiency of the feedstock material [4], [9].
In the context of multi-material additive manufacturing via PBF-LB/M, CuCr1Zr was printed on tool steel 1.2344, employing a process parameter transition approach. The study utilized three transitional zones in CuCr1Zr to enhance fusion from 1.2344 to CuCr1Zr. The volumetric energy density (VED) was adjusted incrementally, starting from 57.3 J/mm³ in the steel region and increasing progressively through the transitional zones to 57.3 J/mm³, 124.6 J/mm³, 192 J/mm³ and finally 259.3 J/mm³ for bulk CuCr1Zr [10].
Mechanical testing of the as-built samples revealed a yield strength of 212 MPa and an ultimate tensile strength of 239 MPa. Post-processing via direct aging heat treatment resulted in the highest recorded strength values, with yield strength reaching 237 MPa and ultimate tensile strength reaching 304 MPa. In contrast, solution-treated and solution-aged samples halved in yield strength values, while ultimate tensile strength remained largely unchanged relative to the as-built samples. Fractography analysis identified two primary failure locations: within the bulk CuCr1Zr and at the interface between CuCr1Zr and tool steel 1.2344. The presence of flat, copper-lined fracture surfaces indicated brittle failure within the CuCr1Zr regions. Notably, the achieved yield- and ultimate tensile strength did not show a significant correlation with the failure location. Cross-sectional investigations also revealed contamination, underscoring the importance of proper machine maintenance and sample cleaning in PBF-LB/M multi-material manufacturing [10]. The study demonstrated that incorporating transition zones to gradually adjust VED is an effective method to minimize intermixing zone height and mitigate hot cracking in multi-material PBF-LB/M [10].

In a study additive manufacturing M300/CuCr1Zr, thermal properties were studied of the successfully manufactured part. The study concluded that due to the CuA-based multi-material parts having a dense cross-section, one-step multi-material PBF-LB/M is comparable to single material PBF-LB/M. The study reached value increase in thermal diffusivity by 150% of the multi-material part compared to pure M300 [11].

3.1.2 Cu10Sn

Cu10Sn has been successfully combined with Ti6Al4V [6], and 316L [3], [12], [13], [14], through PBF-LB/M additive manufacturing.

In a study on 316L/Cu10Sn multi-material fabrication, dense 10 × 10 × 6 mm parts were produced with three transitional zones and good interfacial bonding. The microhardness in the interface exhibited a gradual decrease from 329.5 HV ± 12.5 HV from the 316L region to 172.8 HV ± 7.4 HV to the Cu10Sn region [13].

The ultimate tensile strength and flexural strength of the manufactured part reached values between 316L and Cu10Sn. Notably, the shear stress of the multi-material sample reached 210 MPa, surpassing that of steel/copper alloys manufactured using conventional techniques such as welding, hot-rolling, and compound casting [13]. Mechanical testing confirmed strong interfacial bonding, with the ultimate tensile strength of the multi-material specimens exceeding that of pure Cu10Sn samples. Additionally, the specimens demonstrated high resistance to torsional stress in both bending and shear direction [13].

Two studies investigated the effects of combined island- and interlayer-staggered scanning strategies on 316L/Cu10Sn fabrication [3], [14].

One study focused on processing parameters and particularly their effect on interfacial protrusions, which were analyzed across 25 experimental conditions. The measured protrusion heights ranged from 430.23 ± 24.18 μm to 77.51 ± 8.32 μm while the applied VED varied between 231.11 J/mm^3 and 122.81 J/mm^3 [3]. The study found that increasing VED initially led to a rise in protrusion height, followed by a subsequent decrease. These interfacial protrusions were attributed to the differences in heat transfer coefficients between 316L and Cu10Sn. Among the VED parameters, scanning speed had the most significant influence on protrusion formation [3].

At the interface, insufficient VED led to incomplete melting, resulting in horizontal cracks and voids, whereas excessive VED caused vertical microcracks and porosity. These findings underscore the importance of optimizing energy input to achieve defect-free interfaces in multi-material additive manufacturing [3]. Tensile testing of the fabricated samples yielded an optimal ultimate tensile strength of 459.54 ± 3.08 MPa with an elongation of 5.23 ± 0.65%. In contrast, the minimum recorded joint ultimate tensile strength in the experiment was 199.02 ± 0.56 MPa, with a significantly lower elongation of 1.70 ± 0.22% [3].

3.2 Pre-processing Considerations

3.2.1 Processing parameters & Energy density considerations (VED)

One of the most critical factors in fabricating high-quality parts via PBF-LB/M is the scan strategy**,** including careful adjustment of laser power, scanning speed, and hatch spacing in accordance with the specific material and geometry of the part being manufactured [15]. In certain cases, applying laser remelting (LR) has shown promise in achieving a continuous gradient at the interface and thus a high-quality part [4], [16].

The use of machine learning has been proposed as a promising approach to predict optimal processing parameters based on the material system, allowing for more efficient and accurate process planning, more of which is discussed in chapter 3.3.1 [17].

Processing parameters are also key determinants of the interfacial microstructure, width of the mixing zone, and extent of defect zones in multi-material PBF-LB/M parts. These factors directly affect the mechanical and functional performance of the printed components. [11].
While VED has often been used as a measure to evaluate process quality, its reliability remains debated. VED is a thermodynamic quantity that does not fully capture the complex physical phenomena occurring during melting, such as Marangoni convection which is a key fluid dynamic effect in the melt pool [18]. Nonetheless, VED can still serve as a useful indicator for estimating the manufacturability of a part. In multi-material manufacturing, Marangoni convection has been identified as a dominant mechanism driving the melt pool behaviour and is responsible for the stir-induced bonding between dissimilar materials [16].

3.2.2 Material transition gradients and joints

When bonding materials with significantly different thermal conductivities and interfacial properties, specific strategies must be employed to ensure strong joint integrity. Even in the absence of an additional bonding material, some direct metal combinations can form stable joints due to inherent intermixing phenomena [7].
In a study experimenting with different hierarchical interlocking interfaces between multi-materials via PBF-LB/M, 3D IN718/CuCrZr multi-materials were printed. Two different joints were compared to a flat interfaced sample. Mechanical properties testing showed that the design can improve stress distribution and bonding at the interface. The study concluded that a interfacial joint can increase the contact area and likelihood of mixing between dissimilar materials at the interface [19].

3.2.3 Deposition sequence

In a study on M300/CuCrZr multi-material parts, deposition sequence showed to be important due to differences on thermal properties of the two materials [11]. When process parameters suited for making dense single-material parts were used in multi-material interface parameters in printing M300 on CuCrZr, interfacial defects occured. This indicated the energy input to be insufficient due to CuCrZr below the interface [11].

Additionally, the contents of an article manufacturing CoCrMo/18Ni300/CuSn10/316L parts, the study concurred that the material with a higher thermal expansion coefficient being last to deposit, might reduce residual stress accumulation during the PBF-LB/M process [7]. Taking the difference of thermal properties of base materials into account, it shows importance to strategize the influence of processing parameters and deposition sequence [11].

3.3 In Situ Monitoring & Quality Control

3.3.1 High-speed camera tracking & machine learning

Machine learning was proposed to be an inexpensive way to track in situ progression to a range of PBF processes including PBF-LB/M. A study tracked defect detection accuracy of 85% for single-material samples with an ensemble classifier, which could be integrated with other monitoring systems or sensor modalities to better accuracy [17]. This could be beneficial in investigating process parameters further in PBF-LB/M CuA-based multi-material fabrication.

3.3.2 Laser remelting for defect reduction

Laser remelting (LR) is a process where a rescan with the laser is applied after initial laser scan without added material [8], [20]. LR application can be necessary to enhance the mixing degree in a controlled manner without lowering the quality of the manufactured part [21]. In some cases, surface roughness and porosity can also be improved by applying LR [5], [16].
Investigating the interface in a study of Cu10Sn and Ti6Al4V bonding, remelting Cu10Sn allowed it to enter excessive keyhole mode [6]. Due to entering keyhole mode, the mixing of Ti6Al4V and Cu10Sn intensified as it created two separate TiA-CuA phases which again intermixed, leading better bonding between the materials. The two phases displayed no interface defects internally or between the Ti base material. Instead, narrow vertical voids could be found in the sidewalls of the keyhole and the TiA base material due to keyhole not being fully refilled with liquid metal [6].

While manufacturing CuCr1Zr on M300 steel, remelting with a 90° rotation was applied on CuCr1Zr manufacturing to ensure stable manufacturing manner and high density [11]. When observing the summary of defect density, CuCr1Zr on M300 parts with applied remelting on the interfacial layers shows effects of defect density decrease. Two parts were manufactured with a laser power of 500W and scanning speed of 600 mm/s, one with applied remelting with scanning speed of 750 mm/s. In total, defect density decreased from 0.61% to 0.51%. With remelting applied, defect density of 0.04% was achieved on a CuCrZr on M300 steel multi-material part [11].

3.4 Post-processing techniques

According to literature some of the best ways to improve PBF-LB/M manufactured CuA-based multi-material parts is via hot isostatic pressing (HIP) treatment or direct age hardening (DAH) [4], [11], [15]. In some cases, annealing treatment (AT) was studied [22]. Post-heat treatments in general are key in manufacturing CuA-based multi-material parts with low to none porosity and improved properties.

3.4.1 Hot isostatic pressing (HIP)

Hot isostatic pressing is a post processing heat treatment technique to improve relative density [23]. The process involves subjecting the material to high temperature and isostatic gas pressure (typically using inert gases) within a sealed chamber [23]. This combination of heat and pressure can eliminate internal voids, reduce porosity, and enhance the bonding between particles or layers in additively manufactured materials [23].

The HIP treatment has been shown to greatly reduce porosity in CuA-based multi-material parts [4], [16]. E.g when leaving a gap of unmelted CuCrZr in the interface of 316L/CuCrZr manufactured parts, HIP treated specimens showed no noticeable differences in quality when comparing to a part with fully melted layer [24]. Making it a viable alternative for DAH, discussed more on chapter 3.4.2. HIP treatment was also found as an effective way in closing numerous cracks and pores that are visible in the vicinity of the interfaces. It also showed to increase hardness in the transition zone and in rest of bulk CuCrZr, a decrease in hardness was noticed.

3.4.2 Age Hardening (AH)

Age hardening (commonly spoken as precipitation hardening or particle hardening) is a post processing heat treatment where the material is heated to a specific high temperature where certain elements are soluble for long periods of time. This allows for fine particles to precipitate and hinder the movement of dislocations thereby enhancing its mechanical properties.

In a study heat treating a PBF-LB/M processed multi-metallic M300 / CuCrZr part to 520°C for 1 h, a one-step AH was shown to increase the average microhardness from HV 450 to HV 600 in M300 and HV 100 to HV 200 in CuCr1Zr. The heat treatment also showed to decrease the transition zone and strain localization in the mixing zone. The bimetallic parts had a dense cross-section, implying that the present one-step multi-material is comparable to single-material parts produced by PBF-LB/M [11]. AH also showed an increase in yield- and ultimate tensile strength while reducing ductility and elongation to failure when manufacturing 1.2344/CuCrZr parts [10].

4 Evaluating material quality and defects

The primary challenges in the fabrication of multi-metallic components are interfacial qualities, particularly concerning material quality and mechanical performance (e.g., tensile and yield strength) are the formation of porosity, delamination and cracking. Out of 6 cases of interfacial production showcased in Table 2. and their respective mechanical qualities at said interface in Table 3, both of which discussed more on section 4.1

4.1 Case analysis

In tables 2 and 3 are gathered six versatile cases of manufacturing CuA-based multi-materials via PBF-LB/M. Cases have been selected via having information on processing strategies and mechanical testing.

Case no. 1 shows a study fabricating Cu10Sn/316L specimens using varying laser powers (300–500 W) and scanning speeds (400–600 mm/s) with a 67° interlayer rotation strategy. Optimal mechanical properties were achieved at 300 W and 500 mm/s, yielding the highest ultimate tensile strength of 617.9 ± 43.4 MPa and elongation of 3.7 ± 0.7%. Strong interfacial bonding was also observed at 400 W and 500 mm/s [13].

Case no. 2 investigated Cu10Sn/316L samples utilizing a staggered island scanning strategy, with optimized parameters of 300 W and 800 mm/s. This configuration achieved a ultimate tensile strength of 459.54 ± 3.08 MPa and elongation of 5.23 ± 0.65% [3].

Case no. 3. printed Cu10Sn/316L specimens at an angle relative to the substrate using the same parameters as Case 2 (300 W, 800 mm/s). The best performance was recorded at a 30° print angle, resulting in a ultimate tensile strength of 562.9 MPa and elongation of 4.96%. Liquid metal embrittlement induced microcracks had little impact on interfacial bonding according to the study. Surface roughness improvements were also noted [25].

Both cases no. 4 and no. 5 cases investigated 2D multi-material printing of CuCrZr/ 316L using 375W laser power and 700 mm/s scanning speed. The coupon in case 5 was printed horizontally on the substrate, resulting in increased contact area compared to the vertical interface in Case 4. This geometric variation was used to evaluate interface influence on bonding [26].

in Case no. 6 a C18400/316L specimen was produced using an island scanning strategy with 300 W laser power and 400 mm/s scanning speed. The copper alloy layer was rescanned to ensure sufficient melting. Mechanical testing revealed failure on the C18400 side, indicating that interfacial bonding strength exceeded that of the printed copper itself [27].

No.	CuA / MTL	P (W)	v (mm/s)	h (mm)	T (mm)	VED (J/mm³)	Scan strategy	
1.	Cu10Sn / 316L	300	500	0.12	0.05	133.3	Interlayer rotation (67°)	[13]
2.	Cu10Sn / 316L	300	800	0.075	0.03	166.7	Interlayer staggered + Island	[3]
3.	Cu10Sn / 316L	300	800	0.075	0.03	166.7	not documented	[25]
4.	CuCrZr / 316L	375	700	0.08	0.03	223.2	Interlayer rotation (67°), multitrack	[26]
5.	CuCrZr / 316L	375	700	0.08	0.03	223.2	Interlayer rotation (67°), multitrack	[26]
6.	C18400 / 316L	300	400	0.15	0.05	100	Island	[27]

Table 2. Numbered copper alloy based multi-material combinations (CuA/MTL) with respective process parameters listed (Laser power P, scanning speed v, hatch distance h, layer thickness T, volumetric energy density VED and scanning strategy)

No.	UTS (MPa)	Elongation (%)	Hardness (HV or GPa)	Defects	
1.	617.9 ± 43.4	3.7 ± 0.7	172.8 - 329.5 (HV)	No significant defects or boundaries	[13]
2.	459.54 ± 3.08	5.23 ± 0.65	2.97 ± 0.36 (GPa)	Holes, Cracks	[3]
3.	562.9	4.96	2.88 - 2.09 (GPa)	microcracks on side surface on layer 1-2, no significant defects on 3-5	[25]
4.	318.2 ± 7.2	5.6 ± 0.6	132.8 - 194.9 (HV)	Cracks, Holes	[26]
5.	519.8 ± 6.2	34.2 ± 0.9	132.8 - 194.9 (HV)	Cracks, Holes	[26]
6.	310 ± 18	not documented	256 ± 7 - 72 ± 3 (HV)	porous voids, unmelted particles	[27]

Table 3. Respective mechanical properties of cases in Table 1. such as ultimate tensile strength (MPa), elongation (%), micro- or macrohardness (HV or GPa, respectively) and open worded defects.

4.2 Porosity

Porosity is a critical defect in the additive manufacturing of multi-material components, as it significantly reduces the mechanical performance of the part by lowering its relative density. In the context of multi-material fabrication, porosity becomes especially problematic when incorporating CuA or pure copper where high thermal conductivity and reflectivity necessitate higher laser power during processing. If the processing parameters are not precisely tailored, especially at the interface between dissimilar materials inadequate fusion can exacerbate porosity formation.
Porosity often happens due to Marangoni effect, where entrapped bubbles create defect zones [26].
As previously discussed, process parameters have a substantial influence on the relative density of the final component. Metrics such as VED have been employed to estimate and optimize relative density and porosity by correlating energy input with process outcomes. While these models do not fully account for complex physical interactions, they remain useful tools for guiding parameter selection and improving build quality in multi-material AM.
In many articles, optimized parameters are used for bulk materials, but tailored parameters for interface between the two materials.

4.3 Surface roughness & waviness

In a recent study utilizing machine learning for in situ prediction of process parameters during additive manufacturing, the relationship between VED and surface morphology at the interface, specifically surface roughness and surface waviness was investigated for both 316L stainless steel and pure copper [28]. The results demonstrated a clear inverse correlation between VED and surface roughness, attributed to the formation of larger melt pools that promote smoother surfaces. For 316L, increasing the VED from 32 J/mm^3 to 333 J/mm^3 resulted in a significant reduction in surface roughness, from 13 µm to 1.8 µm. Similarly in copper, VED increased from 76 J/mm^3 to 661 J/mm^3, leading to a decrease in surface roughness from 14 µm to 8 µm [28].
However, an opposite trend was observed for surface waviness at the interface. As VED increased, surface waviness also increased, again due to the influence of larger melt pools. This effect was more pronounced in 316L compared to copper, primarily due to the lower thermal diffusivity of 316L, which facilitates larger and more persistent melt pools. In contrast, copper's higher thermal diffusivity results in faster heat dissipation and smaller melt pool dimensions, thereby moderating the increase in surface waviness [28]. The most pronounced surface waviness was observed in 316L at the highest investigated VED of 331 J/mm^3, where surface roughness was reduced to 1.8 µm, but surface waviness reached a maximum of 172 µm. Large waviness can potentially lead to failure due to powder roller collision [28]. Surface roughness can also be a result of a high VED, when the laser reaches

keyhole mode and evaporates material, which leads to pore formation from a profound Marangoni-effect [21].

Conclusions and further discussion

This literature review analyzed a range of studies focused on the additive manufacturing of copper alloy (CuA) multi-material components. While the feasibility of producing such parts has been demonstrated significant challenges persist, primarily stemming from the low laser absorptivity of CuA materials and the intrinsic dissimilarities between the paired metals, particularly in terms of their mechanical and thermophysical properties.

The main conclusions drawn from the reviewed literature are as follows:

(1) CuA-based multi-materials manufactured via PBF-LB/M are possible to manufacture with dense, almost free-of-defect cross-sections and strong interfacial bonding. This necessitates a comprehensive strategy encompassing all stages of the manufacturing process.

(2) Common manufacturable CuA-based multi-materials include primarily CuSn10 and CuCrZr being paired with steels such as 316L, 1.2344 and M300.

(3) While possible to print multi-materials with no parameter grading, compositional grading or joints; implementing these can help better interfacial bonding. Popular scanning strategies include island scanning and interlayer rotational scanning which can alleviate process induced stresses. In most cases, printing copper alloy latter to the other metal was most popular and printing the part at an angle to the substrate can help alleviate stresses induced in the printing process. Additionally, post-processing heat treatments were shown to significantly improve interfacial bonding strength by reducing residual stresses and minimizing porosity caused by incomplete melting.

(4) For final remarks, more research could be done in future on mechanical properties of wider arrange of CuA-based multi-material combinations manufactured via PBF-LB/M. Additionally, machine learning proposes a viable way to track or predict optimal processing parameters in strategy planning or in-situ defect detection making it a promising area for future research.

Acknowledgments

The use of artificial intelligence was in assistance with the formulation of findings during the writing process. However, AI did not influence the written content or the underlying meaning of the author's work.

References

[1] D. Wang *et al.*, “Recent progress on additive manufacturing of multi-material structures with laser powder bed fusion,” *Virtual and Physical Prototyping*, vol. 17, no. 2, pp. 329–365, Apr. 2022, doi: 10.1080/17452759.2022.2028343.

[2] A. Bandyopadhyay, Y. Zhang, and B. Onuike, “Additive manufacturing of bimetallic structures,” *Virtual and Physical Prototyping*, vol. 17, no. 2, pp. 256–294, Apr. 2022, doi: 10.1080/17452759.2022.2040738.

[3] J. Chen, Y. Yang, C. Song, D. Wang, S. Wu, and M. Zhang, “Influence mechanism of process parameters on the interfacial characterization of selective laser melting 316L/CuSn10,” *Materials Science and Engineering: A*, vol. 792, p. 139316, Aug. 2020, doi: 10.1016/j.msea.2020.139316.

[4] X. Tang, X. Chen, F. Sun, P. Liu, H. Zhou, and S. Fu, “The current state of CuCrZr and CuCrNb alloys manufactured by additive manufacturing: A review,” *Materials & Design*, vol. 224, p. 111419, Dec. 2022, doi: 10.1016/j.matdes.2022.111419.

[5] C. Wei, L. Li, X. Zhang, and Y.-H. Chueh, “3D printing of multiple metallic materials via modified selective laser melting,” *CIRP Annals*, vol. 67, no. 1, pp. 245–248, Jan. 2018, doi: 10.1016/j.cirp.2018.04.096.

[6] C. Wei *et al.*, “Cu10Sn to Ti6Al4V bonding mechanisms in laser-based powder bed fusion multiple material additive manufacturing with different build strategies,” *Additive Manufacturing*, vol. 51, p. 102588, Mar. 2022, doi: 10.1016/j.addma.2021.102588.

[7] D. Wang *et al.*, “Interface microstructure and mechanical properties of selective laser melted multilayer functionally graded materials,” *J. Cent. South Univ.*, vol. 28, no. 4, pp. 1155–1169, Apr. 2021, doi: 10.1007/s11771-021-4687-9.

[8] I. Meyer, M. Oel, T. Ehlers, and R. Lachmayer, “Additive manufacturing of multi-material parts – Design guidelines for manufacturing of 316L/CuCrZr in laser powder bed fusion,” *Heliyon*, vol. 9, no. 8, p. e18301, Aug. 2023, doi: 10.1016/j.heliyon.2023.e18301.

[9] P. Lassègue *et al.*, “Laser powder bed fusion (L-PBF) of Cu and CuCrZr parts: Influence of an absorptive physical vapor deposition (PVD) coating on the printing process,” *Additive Manufacturing*, vol. 39, p. 101888, Mar. 2021, doi: 10.1016/j.addma.2021.101888.

[10] E. Uhlmann and Y. Saber, “Mechanical properties of steel–copper multi-material samples built by laser powder bed fusion using a graded energy input,” *Prog Addit Manuf*, vol. 10, no. 1, pp. 475–489, Jan. 2025, doi: 10.1007/s40964-024-00636-7.

[11] X. Li, D. Sukhomlinov, and Z. Que, “Microstructure and thermal properties of dissimilar M300-CuCr1Zr alloys by multi-material laser-based powder bed fusion,” *Int J Miner Metall Mater*, vol. 31, no. 1, pp. 118–128, Jan. 2024, doi: 10.1007/s12613-023-2747-x.

[12] J. Chen, Y. Yang, Y. Bai, D. Wang, C. Zhao, and J. Ying Hsi Fuh, “Single and multiple track formation mechanism of laser powder bed fusion 316L/CuSn10 multi-material,” *Materials Characterization*, vol. 183, p. 111654, Jan. 2022, doi: 10.1016/j.matchar.2021.111654.

[13] K. Chen *et al.*, “Selective laser melting 316L/CuSn10 multi-materials: Processing optimization, interfacial characterization and mechanical property,” *Journal of Materials Processing Technology*, vol. 283, p. 116701, Sep. 2020, doi: 10.1016/j.jmatprotec.2020.116701.

[14] J. Chen, Y. Yang, C. Song, M. Zhang, S. Wu, and D. Wang, “Interfacial microstructure and mechanical properties of 316L /CuSn10 multi-material bimetallic structure fabricated by selective laser melting,” *Materials Science and Engineering: A*, vol. 752, pp. 75–85, Apr. 2019, doi: 10.1016/j.msea.2019.02.097.

[15] C. Wallis and B. Buchmayr, “Effect of heat treatments on microstructure and properties of CuCrZr produced by laser-powder bed fusion,” *Materials Science and Engineering: A*, vol. 744, pp. 215–223, Jan. 2019, doi: 10.1016/j.msea.2018.12.017.

[16] A. Schmidt, F. Jensch, and S. Härtel, “Multi-material additive manufacturing-functionally graded materials by means of laser remelting during laser powder bed fusion,” *Front. Mech. Eng.*, vol. 18, no. 4, p. 49, Dec. 2023, doi: 10.1007/s11465-023-0765-z.

[17] C. Gobert, E. W. Reutzel, J. Petrich, A. R. Nassar, and S. Phoha, “Application of supervised machine learning for defect detection during metallic powder bed fusion additive manufacturing

using high resolution imaging.," *Additive Manufacturing*, vol. 21, pp. 517–528, May 2018, doi: 10.1016/j.addma.2018.04.005.

[18] U. Scipioni Bertoli, A. J. Wolfer, M. J. Matthews, J.-P. R. Delplanque, and J. M. Schoenung, "On the limitations of Volumetric Energy Density as a design parameter for Selective Laser Melting," *Materials & Design*, vol. 113, pp. 331–340, Jan. 2017, doi: 10.1016/j.matdes.2016.10.037.

[19] L. Liu *et al.*, "Laser additive manufacturing of multimaterials with hierarchical interlocking interface via a flexible scraper-based method," *International Journal of Machine Tools and Manufacture*, vol. 205, p. 104236, Feb. 2025, doi: 10.1016/j.ijmachtools.2024.104236.

[20] Z. Yu *et al.*, "Effect of laser remelting processing on microstructure and mechanical properties of 17-4 PH stainless steel during laser direct metal deposition," *Journal of Materials Processing Technology*, vol. 284, p. 116738, Oct. 2020, doi: 10.1016/j.jmatprotec.2020.116738.

[21] D. Dai and D. Gu, "Thermal behavior and densification mechanism during selective laser melting of copper matrix composites: Simulation and experiments," *Materials & Design*, vol. 55, pp. 482–491, Mar. 2014, doi: 10.1016/j.matdes.2013.10.006.

[22] J. Chen, G. Bi, D. Zhao, D. Wang, M. Zhang, and Y. Xiao, "Subsequent enhancement of mechanical properties using heat treatment of steel/copper bimetallic structures manufactured by laser powder bed fusion," *Journal of Materials Research and Technology*, vol. 33, pp. 8944–8957, Nov. 2024, doi: 10.1016/j.jmrt.2024.11.213.

[23] H. V. Atkinson and S. Davies, "Fundamental aspects of hot isostatic pressing: An overview," *Metall Mater Trans A*, vol. 31, no. 12, pp. 2981–3000, Dec. 2000, doi: 10.1007/s11661-000-0078-2.

[24] L. Deillon, N. Abando Beldarrain, X. Li, and M. Bambach, "Coupling hot isostatic pressing and laser powder bed fusion: A new strategy to manufacture defect-free CuCrZr-316L steel multi-material structures," *Materials & Design*, vol. 241, p. 112914, May 2024, doi: 10.1016/j.matdes.2024.112914.

[25] J. Chen *et al.*, "The impact of interfacial characteristics on the interfacial properties of 316 L/CuSn10 multi-material manufactured by laser powder bed fusion," *Materials Characterization*, vol. 211, p. 113862, May 2024, doi: 10.1016/j.matchar.2024.113862.

[26] S. Mao, D. Z. Zhang, Z. Ren, G. Fu, and X. Ma, "Effects of process parameters on interfacial characterization and mechanical properties of 316L/CuCrZr functionally graded material by selective laser melting," *Journal of Alloys and Compounds*, vol. 899, p. 163256, Apr. 2022, doi: 10.1016/j.jallcom.2021.163256.

[27] Z. H. Liu, D. Q. Zhang, S. L. Sing, C. K. Chua, and L. E. Loh, "Interfacial characterization of SLM parts in multi-material processing: Metallurgical diffusion between 316L stainless steel and C18400 copper alloy," *Materials Characterization*, vol. 94, pp. 116–125, Aug. 2014, doi: 10.1016/j.matchar.2014.05.001.

[28] B. Rankouhi, S. Jahani, F. E. Pfefferkorn, and D. J. Thoma, "Compositional grading of a 316L-Cu multi-material part using machine learning for the determination of selective laser melting process parameters," *Additive Manufacturing*, vol. 38, p. 101836, Feb. 2021, doi: 10.1016/j.addma.2021.101836.